Korean J. Chem. Eng., 35(8), 1748-1755 (2018)
DOI: 10.1007/s11814-018-0080-2

pISSN: 0256-1115
eISSN: 1975-7220

Polypropylene surface with antibacterial property by photografting 1-vinylimidazole and subsequent chemical modification

Choon Ki Na*, Ga-Yeon Park*, and Hyunju Park,†**

*Department of Environmental Engineering, Mokpo National University, Jeonnam 58554, Korea
**Institute of Construction and Environmental Engineering, Seoul National University,
1 Gwanak-ro, Gwanak-gu, Seoul 08826, Korea
(*Received 19 February 2018 • accepted 10 May 2018*)

Abstract−The surface of polypropylene (PP) fiber was modified by UV-induced graft polymerization of 1-vinylimidazole (Vim), followed by quaternization with iodomethane, sulfonation with chlorosulfonic acid, or loading of silver (Ag) nanoparticles to endow the surface with antibacterial properties. The modified PP fibers were characterized by FT-IR, SEM, and surface charge analyses. The antibacterial activity of the modified PP fibers was assessed against the Gram-negative and Gram-positive bacteria, *Escherichia coli* (*E. coli*), and *Staphylococcus aureus* (S. *aureus*), respectively. The PP-g-Vim was greatly improved by loading of Ag nanoparticles (≥99.9%), quaternization (98.9-99.2%), or sulfonation (≥99.9%).

Keywords: Polypropylene, Photopolymerization, Modification, Surfaces

INTRODUCTION

As the demand for advanced treatments has been increasing in the water treatment industry, physicochemical separation technologies such as membrane filtration, reverse osmosis, and adsorption separation have come into wide use. Accordingly, development of functional filtering materials is the core of the growth in the water treatment industry as the demand for these materials has been steadily increasing every year. A common problem encountered is "biofouling," which results from the attachment and propagation of microorganisms on the surface during operation [1]. Biofouling reduces the separation efficiency, which, in turn, increases the maintenance and/or operation costs. Therefore, attempts to endow the surfaces with antibacterial properties by physio-chemical methods, such as blending, coating, crosslinking, and graft copolymerization, have received considerable attention [2,3].

Two principal strategies have been investigated to construct the antibacterial surfaces: (1) incorporating inorganic nanoparticles such as silver (Ag) [4-6], TiO_2 [7,8], and Al_2O_3 [9] into the polymer matrix or immobilizing them onto the surface; and (2) introducing organic compounds with antibacterial properties, such as quaternary ammonium compounds [10-12], zwitterionic polymers [13-15], and guanidine compounds [16,17], on the polymer surface. Among the above-mentioned materials, Ag nanoparticles and quaternary ammonium compounds seem to be the most widely used for constructing antibacterial surfaces because of their superior biocidal ability [4-6].

Some imidazole compounds are known to possess antibacterial, antifungal, and antiprotozoal activities [18]. In addition, imidazole-containing polymers have high biocompatibility and are thus considered useful materials for biomedical applications [19]. Furthermore, like other vinyl monomers, vinyl imidazoles can be readily graft-copolymerized with various polymers. Several previous studies reported the graft copolymerization of vinyl imidazoles onto biomaterials and polymers, such as chitosan [20], carboxymethyl chitosan [21], polypropylene (PP) [22], and nylon [23] and demonstrated their potent antibacterial activities. However, Meléndez-Ortiz et al. recently reported that graft copolymers of N-vinylimidazole on poly(vinyl chloride) catheters, prepared by gamma-ray irradiation, showed no antibacterial activity against *Escherichia coli*. Moreover, the bacteria grew well even after full quaternization of the imidazole ring. However, at a grafting yield above 20%, the copolymers showed a highly effective antibacterial activity against *Staphylococcus aureus*, even without quaternization [24]. Notably, most of the studies on the antibacterial properties of organic materials were limited to gamma-ray grafting and quaternization, and there are no studies on the introduction of other functional groups such as photograft polymerization or sulfonation.

In the present study, the surface of PP fiber was modified by UV-induced graft polymerization of 1-vinylimidazole. Then, quaternization with iodomethane, sulfonation with chlorosulfonic acid, or surface immobilization of Ag ions/nanoparticles was done to enhance the antibacterial activity. The effects of grafting conditions including monomer concentration, UV-irradiation time, reaction temperature, and solvent concentration were investigated in detail. The resulting surface properties were indicated in terms of their surface chemical compositions, morphologies, and surface charge densities. The antibacterial activities of the modified PP surfaces were assessed against both Gram-negative and Gram-positive bacteria, represented by *E. coli* and *S. aureus*, respectively.

†To whom correspondence should be addressed.
E-mail: narjjis@snu.ac.kr, narjjis@hanmail.net

MATERIALS AND METHODS

1. Materials

Non-woven PP fabric (180 g/m^2, Samsung Non-Woven Fabric Co., Korea) was used to indicate the grafting substrate polymer. 1-Vinylimidazole (Vim, 99%, Sigma Aldrich, USA), and benzophenone (BP, Yakuri Pure Chemical Co., Japan) used, respectively, as the monomer and photoinitiator. Methanol (MeOH) and deionized water were used as solvents. Silver nitrate ($AgNO_3$, 99.8%), chlorosulfonic acid (98%), dichloromethane (99%), NaCl, KCl, KH_2PO_4, and Na_2HPO_4 were purchased from commercial suppliers. All chemicals and solvents were of high grade and used as received without any purification. *E. coli* (AATCC 25922) and *S. aureus* (AATCC 6538) were obtained from the Korean Culture Centre of Microorganisms (Seoul, Korea). The Difco™ nutrient broth was purchased from Becton, Dickinson and Company (MD, USA). 3M™ Petrifilm™ plates were used to culture *E. coli* and *S. aureus*.

2. Grafting of Vim onto PP Surface

The non-woven PP fabric was cut into 2×5 cm pieces and dried at 60 °C prior of grafting. The monomer solution was prepared with 5-20 vol% MeOH in water as the solvent and contained 2.5-10.0 vol% Vim and 0.2 wt% BP. One piece of the PP fabric was placed in a Pyrex glass tube containing 20 mL of the monomer solution. The tube was purged with nitrogen gas to eliminate oxygen and sealed. The tube was then exposed to UV light at 60-80 °C for 2-8 h using a 400 W high-pressure mercury lamp (Miya Electric Co., Korea) as the light source. The glass tubes were set to rotate and simultaneously revolve around the source of light at a distance of 10 cm. After the grafting reaction, the samples were taken out from the glass tubes and washed three times with hot water, extracted with MeOH for 3 h in a Soxhlet apparatus to remove unreacted monomer and homopolymer, and then dried at 60 °C until a constant weight was obtained. The degree of grafting was calculated flowing Eq. (1):

$$\text{Degree of grafting (\%)} = \frac{100(W_1 - W_0)}{W_0} \quad (1)$$

where W_0 and W_1 are the weight of the substrate PP fabric and the grafted PP fabric, respectively. At least three parallel experiments were executed for each condition.

3. Quaternization of PP-*g*-Vim

PP-*g*-Vim fabrics with a grafting degree between 25-100% were immersed in 10 vol% iodomethane (CH_3I) solution in MeOH, and sterilized for 5 h at room temperature, protected from light. The quaternized PP-*g*-Vim fabrics (PP-*g*-Vim-CH_3I) were washed with MeOH and deionized water to remove the unreacted CH_3I and dried at 60 °C until a constant weight was obtained. The density of the quaternized imidazole ring was estimated as follows [25]:

$$\text{Density of quaternized imidazole ring (mmol/g)} = \frac{(W_2 - W_1)}{W_2} \times \frac{1000}{149.1} \quad (2)$$

where W_2 represents the weight of the quaternized PP-*g*-Vim fabric, while 141.9 corresponds to the molecular weight of CH_3I [25].

4. Sulfonation of PP-*g*-Vim

PP-*g*-Vim fabrics with a grafting degree between 25-100% were immersed in 5 vol% chlorosulfonic acid in dichloromethane for 1 h at room temperature. After the reaction, the sulfonated PP-*g*-Vim fabrics (PP-*g*-Vim-SO_3H) were washed several times with acetone for removing the unreacted chlorosulfonic acid and dichloromethane and then dried at 60 °C until a constant weight was obtained. The density of the sulfonic acid group was estimated as follows:

$$\text{Density of sulfonic acid group (mmol/g)} = \frac{(W_3 - W_1)}{W_3} \times \frac{1000}{116.5} \quad (3)$$

where W_3 represents the weight of the sulfonated PP-*g*-Vim fabric, while 116.5 corresponds to the molecular weight of $ClSO_3H$.

5. Loading of Ag Ions onto PP-*g*-Vim

PP-*g*-Vim fabrics with a grafting degree between 25-100% were immersed in 1.0 wt% $AgNO_3$ solution dissolved in MeOH and shaken at room temperature for 24 h. The Ag ion-immobilized fabric was then washed with MeOH to remove the residual $AgNO_3$ and then re-immersed in 0.4% $NaBH_4$ solution to reduce the Ag ion immobilized onto the fabric. After shaking for 2 h at room temperature, the fabric was rinsed with deionized water to remove the residual salts, and then dried at 60 °C until a constant weight was obtained. The density of Ag nanoparticles on PP-*g*-Vim was

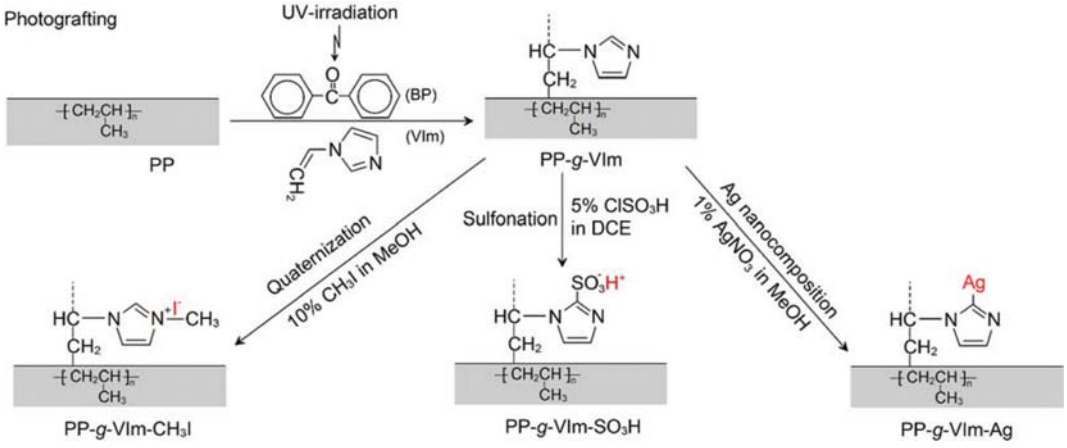

Fig. 1. Schematic illustration of PP surface modification process.

estimated from the weight gain as:

$$\text{Density of Ag nanoparticle (mmol/g)} = \frac{(W_4 - W_1)}{W_4} \times \frac{1000}{107.9} \quad (4)$$

where W_4 represents the weight of the Ag-loaded PP-g-Vim fabric (PP-*g*-Vim-Ag), and 107.9 corresponds to the atomic weight of Ag.

The synthetic route and the chemical structure of PP-g-Vim and further modified PP-g-Vim fabrics are shown in Fig. 1.

6. Characterization of Surface

The chemical structure of the PP-*g*-Vim fabrics was analyzed using a Fourier transform infrared (FT-IR) spectrophotometer (Shimadzu IR-435, Japan). Scanning electron microscopy (SEM, Hitachi S-4800) was used for observing the surface morphology of the PP-*g*-Vim fabrics. The surface charges of the PP-*g*-Vim fabrics were measured using the potentiometric titration method [26]. The fabric was cut into 5×5 mm pieces and then mixed with 0.01 M NaCl solution to obtain a 2 g/L suspension. Titrations were performed by the addition of 0.1 M HCl and 0.1 M NaOH using a micropipette. The pH values of the suspensions were measured using a pH meter (Thermo Scientific Orion 3-Star). The surface charge density, s (C/cm^2), was calculated as a function of pH using Eq. (5):

$$\sigma(\text{C/cm}^2) = \frac{F(C_A - C_B + [OH^-] - [H^+])}{WA} \quad (5)$$

where F is the Faraday's constant (96,490 C/mol), C_A and C_B are the concentrations of the acid or base after each addition during the titration (mol/L), $[H^+]$ and $[OH^-]$ are the equilibrium concentrations of H^+ and OH^- ions, W and A are the weight (g) and the surface area (cm^2/g) of the fabric, respectively.

7. Antibacterial Testing

Antibacterial tests were conducted with *E. coli* and *S. aureus* pure cultures according to previous reports [3,14]. *E. coli* and *S. aureus* were cultivated in a sterilized nutrient medium (containing 10 g/L peptone and 3 g/L beef extract at a pH 6.8) at 37 °C with shaking at 150 rpm for 24 h. The bacterial cultures were harvested by centrifugation at 3,000 rpm for 10 min. The cells were washed twice with sterilized 0.5% saline solution and resuspended in 1/20 nutrient medium. The bacterial cell concentration was estimated from the optical density (OD) at 540 nm, based on a predetermined calibration curve between the OD and cell concentration. A working suspension was prepared by diluting the cells to a concentration of 10^6 cells/mL using the 1/20 nutrient medium. One piece of the original or modified fabric (2×2 cm) was immersed in 5 mL working suspension in a 30 mL sterile glass bottle and incubated at 37 °C for 1 h with continuous shaking. After 1 h, 1 mL of the working suspension was removed, diluted appropriately with saline solution, and 0.5 mL of the diluted solution was spread onto Petrifilm™ plates. After incubation of the plates at 37 °C for 24-48 h, the number of colony-forming units (CFUs) was counted by using a colony counter. The mean CFU/mL was obtained by multiplying the CFU count with the dilution factor. The antibacterial activity of the fabric was calculated as follows:

$$\text{Antibacterial activity (\%)} = \frac{(N_0 - N_t)}{N_0} \times 100 \quad (6)$$

where N_o is the number of CFUs in the control solution (in contact with the substrate PP fabric) and N_t is the number of CFUs in the test solution.

RESULTS AND DISCUSSION

1. Grafting of Vim on PP Fiber

To determine the optimal conditions for photografting, the effects of UV irradiation time, reaction temperature, monomer concentration, and MeOH concentration on the degree of grafting were investigated. Fig. 2(a) shows the effects of varying the UV irradiation time from 2-8 h and the reaction temperature from 60-80 °C at fixed concentrations of the monomer (10 vol%) and MeOH (20 vol%). It is evident that the degree of grafting increased with an increase in the UV irradiation time and the reaction temperature. An increase in the UV irradiation time increases the number of

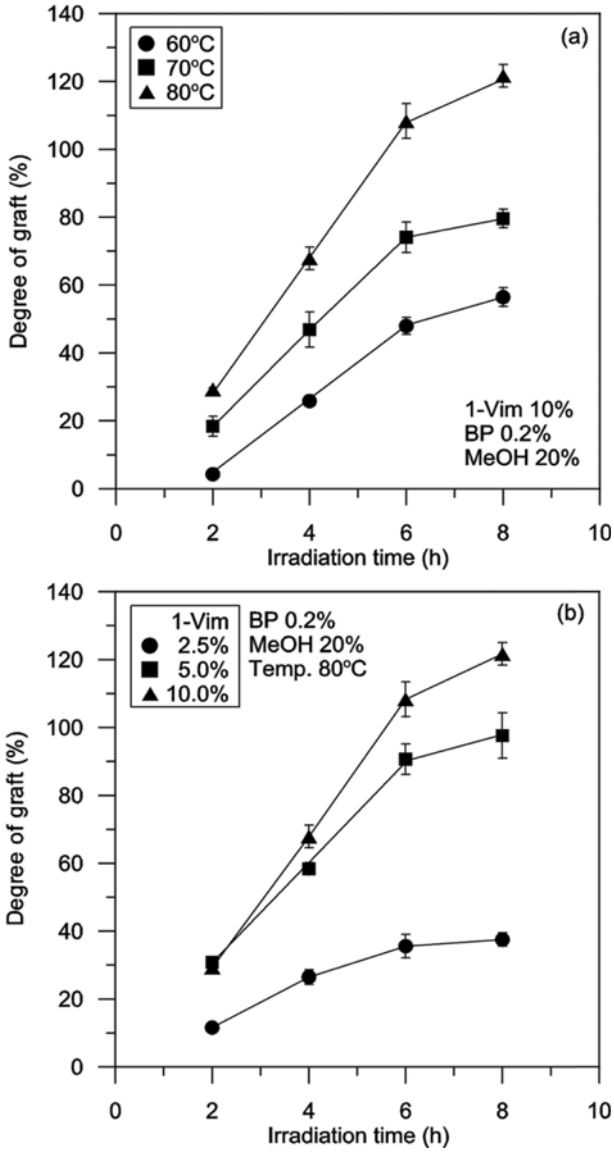

Fig. 2. Effects of photo-irradiation time at various reaction temperature (a) and Vim concentration (b) on the degree of grafting onto PP fiber.

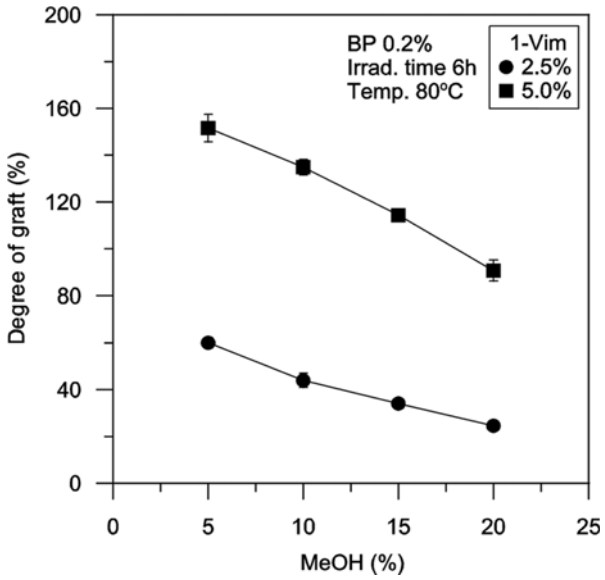

Fig. 3. Effect of MeOH concentration in the monomer solution on the degree of grafting onto PP fiber.

BP molecules that are excited to the triplet state by absorbing the UV energy. Thus, more molecules can abstract hydrogen atoms from the PP surface to yield radicals, which are capable of initiating graft polymerization with the monomers. Irrespective of the reaction temperature, the grafting degree tended to decrease after 6 h of UV irradiation. This is probably due to a large amount of homopolymer formation in the residual monomer solution, which would decrease the amount of monomer that is available for graft polymerization. The increase in the degree of grafting upon increase in the reaction temperature can be explained by the resultant increase in the mobility of the monomer and the diffusion velocity of the photoinitiator, which leads to an increase in the probability of polymerization reactions. Fig. 2(b) shows the changes in the degrees of grafting upon varying the UV irradiation time (2-8 h) and the monomer concentrations (2.5, 5.0, and 10.0%) at a fixed MeOH concentration (20 vol%) and reaction temperature (80 °C). The degrees of grafting were considerably different between 2.5% and 5.0% monomer concentrations, although, irrespective of monomer concentrations, the grafting degree increased with an increase in the UV irradiation time. Fig. 3 shows the effects of varying the concentration of MeOH (5-25%), the solvent for photografting, on the degrees of grafting at two monomer concentrations (2.5 and 5.0%), at a fixed UV irradiation time of 6 h at 80 °C. The degree of grafting showed a clear tendency to increase with a decrease in MeOH concentration. MeOH was essential at an appropriate concentration to dissolve BP, which is water insoluble, in the monomer solution for use as a photoinitiator. However, the decrease in the degree of grafting at such high concentrations might be due to the hydrogen bonding present in MeOH, which is highly reactive to abstraction. Indeed, it is known that the solvent has an effect on the photografting and is directly proportional to the photoreduction reactivity of the hydrogen bonding present in the solvent [27].

2. Activation of Vim Graft Chain

To enhance the antibacterial activity of the grafted copolymers,

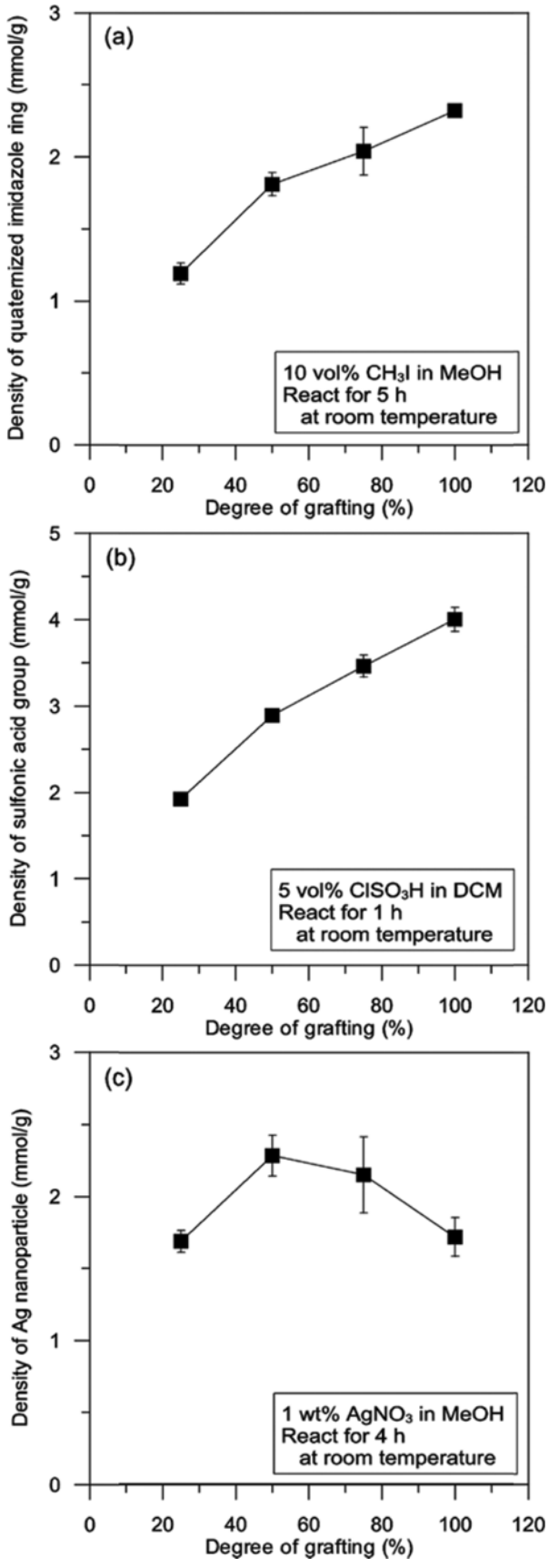

Fig. 4. Densities of CH_3I group (a), SO_3H group (b) and Ag nanoparticles (c) in PP-g-Vim depending on the degree of grafting.

the imidazole group grafted onto the PP surface was subsequently modified by quaternization with iodomethane, sulfonation with chlorosulfonic acid, or loading of Ag ions/nanoparticles. Fig. 4 shows the densities of the methyl iodide group (a), sulfonic acid group (b), and Ag nanoparticles (c) introduced to the Vim graft chains of the PP-*g*-Vim fabric, with the degree of grafting in the range of 25-100%, by quaternization and sulfonation of the PP-*g*-Vim fabric, respectively. As shown in Fig. 4, the iodomethane and sulfonic acid groups showed an increase in the range of 1-4 mmol/g along with the increase of the grafting degree. Unlike these groups, the density of Ag nanoparticles showed a maximum value of 2.5 mmol/g when the degree of grafting was 50% and decreased thereafter (Fig. 4(c)). A similar trend was found in the adsorption capacities of quaternized PP-*g*-Vim-CH_3I and sulfonated PP-*g*-Vim-SO_3H. Fig. 5 shows the PO_4^{3-} and NH_4^+ adsorption capacities of PP-*g*-Vim-CH_3I and PP-*g*-Vim-SO_3H, respectively. As shown, maximum adsorption capacities for PO_4^{3-} and NH_4^+ were reached when the degrees of grafting were 50% and 75%, respectively. Although the densities of the methyl iodide and sulfonic acid groups, which are the functional adsorption groups, increased in proportion to the grafting degree (Fig. 5), their adsorption capacities decreased at high degrees of grafting. This could be because of the thickening of the graft layers by graft polymerization and subsequent modification reactions, which decreased the specific surface areas or inhibited the internal diffusion of ionic substances. Together, these results suggest that appropriate degrees of grafting of Vim for the preparation of antibacterial surfaces would be approximately 50-75%.

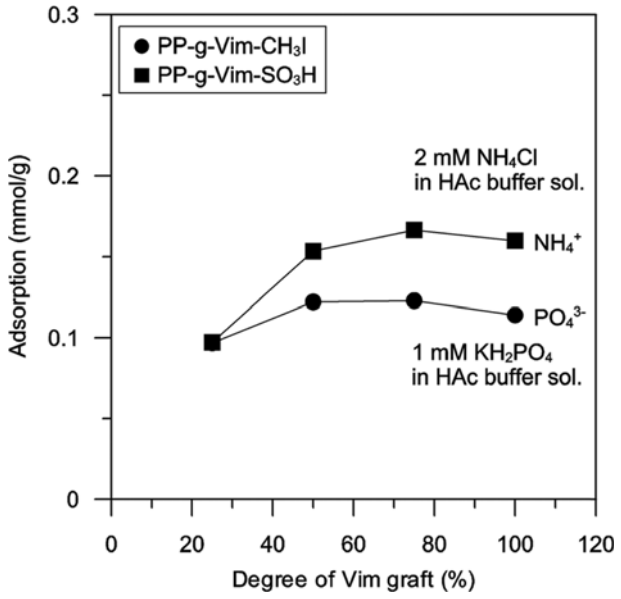

Fig. 5. Effects of the degree of Vim grafting on adsorption capacities of quaternized and solfonated PP-g-Vim.

3. Surface Characterization

The substrate PP, grafted copolymer PP-*g*-Vim, quaternized PP-*g*-Vim-CH_3I, and sulfonated PP-*g*-Vim-SO_3H were subjected to SEM, FT-IR, and surface charge analysis to identify the changes in the surface characteristics and chemical structure of PP due to graft polymerization and the subsequent surface modification reactions.

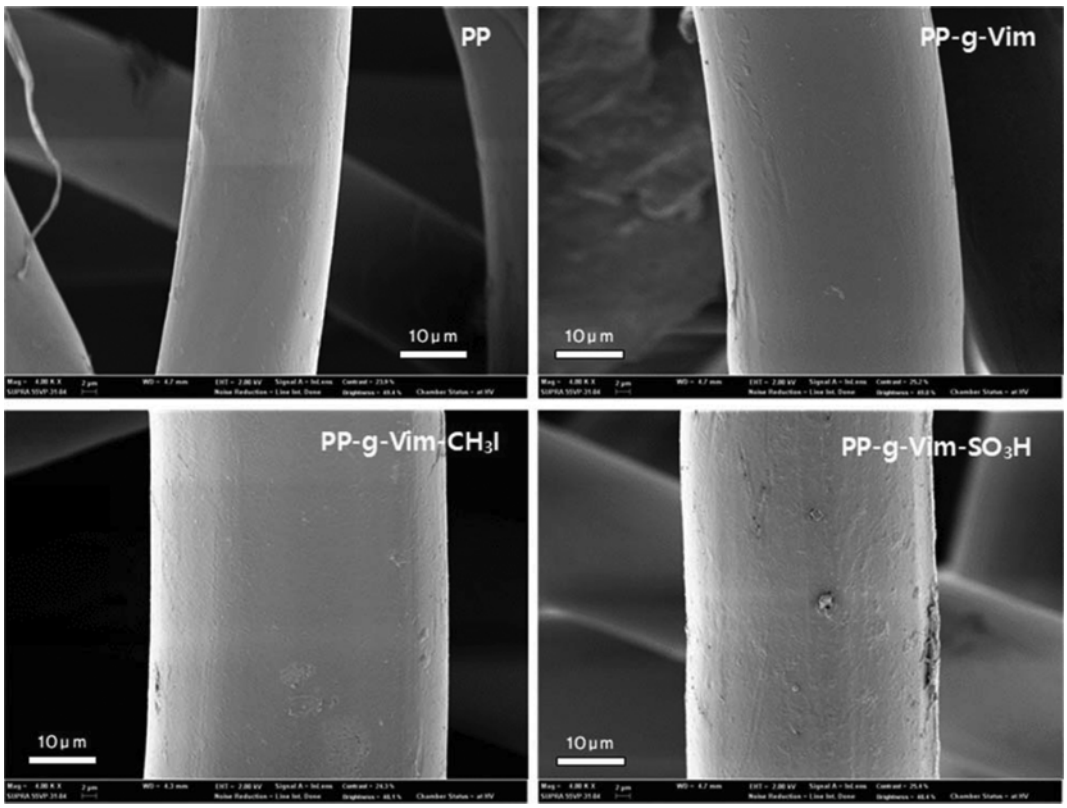

Fig. 6. SEM images of PP, PP-g-Vim, PP-g-Vim-CH_3I, and PP-g-Vim-SO_3H.

As shown in Fig. 6, SEM images of the substrate PP, PP-*g*-Vim, PP-*g*-Vim-CH_3I, and PP-*g*-Vim-SO_3H indicated that graft polymerization and subsequent surface modification reactions led to a thickening of the PP fibers by at least 2-fold.

The FT-IR spectra obtained from the substrate PP, grafted copolymer PP-*g*-Vim, quaternized PP-*g*-Vim-CH_3I, and sulfonated PP-*g*-Vim-SO_3H are presented in Fig. 7. The FT-IR spectrum of the substrate PP included many peaks at 1,375, 1,455, 2,840, 2,870, 2,920, and 2,950 cm^{-1}, which corresponded to the stretching vibrations of the C-H bond in the CH_2 and CH_3 groups [28,29]. In the grafted copolymer PP-*g*-Vim, characteristic peaks were seen at 1,220 cm^{-1} corresponding to the N-C-N bond, and at 1,495 and 1,550 cm^{-1} corresponding to the stretching vibrations of the aromatic C=C and C=N bonds in the imidazole ring, respectively, confirming that Vim was grafted onto the substrate PP polymer. After quaternization with iodomethane and sulfonation with chlorosulfonic acid, new peaks appeared at 1,165 and 1,039 cm^{-1} corresponding to $=N^+$-CH_3 and O=S=O stretching vibrations, respectively, as a result of the appearance of the iodomethane and sulfonic acid group in the PP-*g*-Vim fabrics, indicating the successful preparation of the quaternized PP-*g*-Vim-CH_3I and the sulfonated PP-*g*-Vim-SO_3H fabrics [30].

Fig. 8 shows the surface charge densities of the various fabrics. While the substrate PP shows surface charges close to 0 irrespective of the pH, the surface charge of PP-*g*-Vim varies with the pH, showing an increase in the positive and negative values in the acidic and alkaline ranges, respectively. The surface charges of the quat-

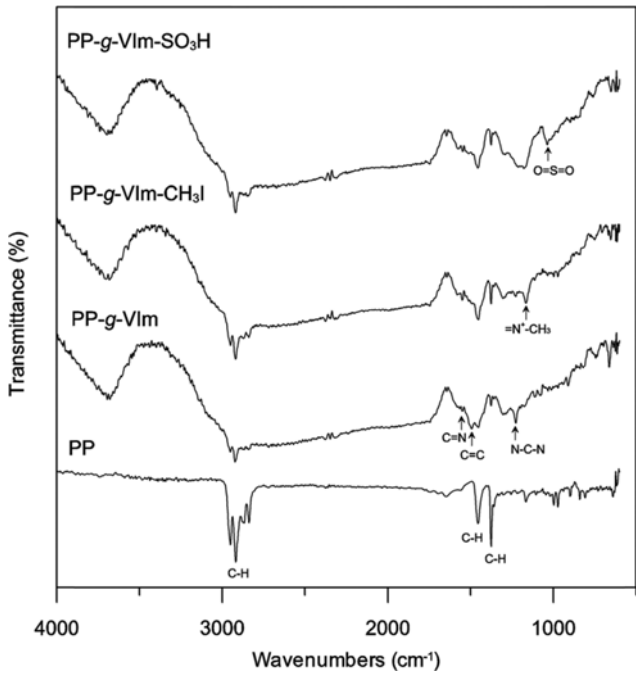

Fig. 7. FT-IR spectra of PP, PP-g-Vim, PP-g-Vim-CH_3I, and PP-g-Vim-SO_3H.

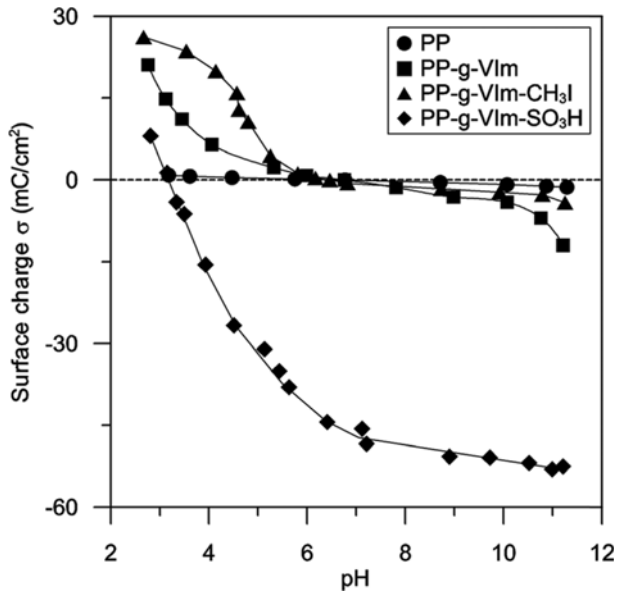

Fig. 8. Surface charge density of PP, PP-g-Vim, PP-g-Vim-CH_3I, and PP-g-Vim-SO_3H as a function of pH.

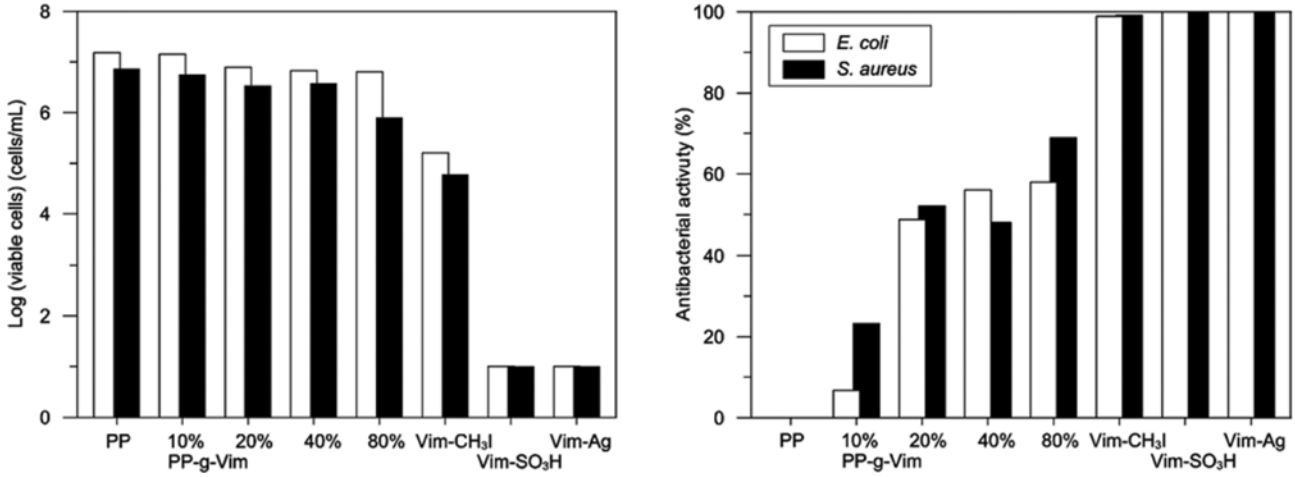

Fig. 9. Viable cell numbers and antibacterial activities of *E. coli* and *S. aureus* after contact with PP-g-Vim fibers depending on the degree of grafting and subsequent surface modification methods.

ernized PP-*g*-Vim-CH_3I became more positive along with decreasing pH, while those of sulfonated PP-*g*-Vim-SO_3H became more negative with increasing pH. These results indicate that the surfaces of these fabrics acquired positive potentials (anion-exchange capacity) and negative potentials (cation-exchange capacity) by quaternization and sulfonation, respectively.

4. Antibacterial Properties

The antibacterial activity of PP-*g*-Vim, PP-*g*-Vim-CH_3I, PP-*g*-Vim-SO_3H, and PP-*g*-Vim-Ag against *E. coli* (indicating for Gram-negative microorganism) and *S. aureus* (indicating for Gram-positive microorganism) was evaluated. As shown in Fig. 9, PP-*g*-Vim exhibited 6.7-58.0% and 23.3-69.2% antibacterial activities against *E. coli* and *S. aureus*, respectively, as the grafting degree rises in the range of 10-80%, indicating that imidazole groups possess antibacterial property. However, the antibacterial activities of PP-*g*-Vim did not exceed 70% compared to that of the substrate PP, indicating that their antibacterial activity was not optimal. Meanwhile, when the grafted imidazole group (50±5% degree of grafting) was quaternized (-CH_3I), sulfonated (-SO_3H), or Ag ions were introduced to the graft chains, the antibacterial activities remarkably improved, reaching 98.9%, ≥99.9%, and ≥99.9% against *E. coli* and 99.2%, ≥99.9%, and ≥99.9% against *S. aureus*, respectively. In particular, PP-*g*-Vim-SO_3H, with the sulfonic acid group, and PP-*g*-Vim-Ag, with Ag nanoparticles, showed a very high germicidal power as indicated by the drastic reduction in the bacterial cell count from 10^6 CFU/mL to less than 10 CFU/mL after contact of the culture with the test solutions of these fabrics. From these results, it can be seen that the antibacterial activity of only the Vim-grafted polymers was limited and to obtain high antibacterial activity, the imidazole group grafted onto the substrate polymer had to be further modified by quaternization, sulfonation, or loading of Ag ions, which reinforced the antibacterial functionality of these surfaces.

To evaluate the reusability of the PP-*g*-Vim and further modified fibers, the fibers after being used for antibacterial test were regenerated by washing with ethanol and drying at 60 °C. The reuse cycle was repeated ten times and the antibacterial activity against *E. coli* was measured for each cycle. As shown in Fig. 10, the antibacterial activity of PP-g-Vim decreased with the number of reuse cycles. After using for the fifth time, the antibacterial activity decreased down to less than 10% and then disappeared. However, further modified PP-*g*-Vim fibers by quaternization, sulfonation, or loading of Ag ions exhibited almost constant antibacterial activity regardless of the number of reuse cycles. The results suggest that the imidazole group grafted onto the substrate polymer should be further modified to obtain a high antibacterial activity and durability.

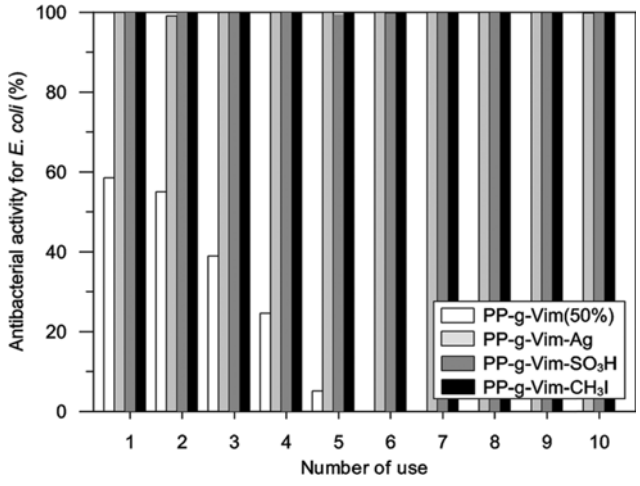

Fig. 10. Evaluation of the reusability of PP-g-Vim, PP-g-Vim-CH_3I, and PP-g-Vim-SO_3H and PP-g-Vim-Ag fibers.

CONCLUSIONS

PP surfaces were modified by UV-induced graft copolymerization of Vim and then by quaternization with iodomethane, sulfonation with chlorosulfonic acid, or loading of Ag nanoparticles.

The degree of Vim grafting was influenced by the monomer concentration, irradiation time, reaction temperature, and the content of MeOH as a solvent. A concentration of 5-10% Vim, a UV irradiation time of 4-6 h, a reaction temperature of 80 °C, and a concentration of 20% MeOH seems to be optimal for the grafting of Vim onto PP in terms of a stable degree of grafting.

The antibacterial activity of the PP-*g*-Vim fabric against both *E. coli* and *S. aureus* was shown to be below 70%, indicating that additional surface modification was necessary to enhance their antibacterial activity. When PP-*g*-Vim was quaternized with iodomethane, sulfonated with chlorosulfonic acid, or its surface loaded with Ag nanoparticles, the antibacterial activities against both *E. coli* and *S. aureus* were enhanced substantially (>99%). The antibacterial activity against both *E. coli* and *S. aureus* increased in the order of PP-*g*-Vim-Ag>PP-*g*-Vim-SO_3H>PP-*g*-Vim-CH_3I>PP-*g*-Vim. Further, modified PP-*g*-Vim fibers exhibited superior durability in the antibacterial activity.

ACKNOWLEDGEMENTS

This research was supported by the National Research Foundation of Korea (NRF) funded by the Ministry of Education, Science and Technology (NRF-2015R1C1A2A01052334).

REFERENCES

1. J. W. Costerton, P. S. Stewart and E. P. Greenberg, *Science*, **284**, 1318 (1999).
2. Y. Wang, T. Wang, Y. Su, F. Peng, H. Wu and Z. Jiang, *Langmuir*, **21**, 11856 (2005).
3. Y. Chiag, Y. Chang, W. Chen and R. Ruaan, *Langmuir*, **28**, 1399, (2012).
4. C. X. Liu, D. R. Zhang, Y. He, X. S. Zhao and R. Bai, *J. Membr. Sci.*, **346**, 121 (2010).
5. X. Ping, M. Wang and X. Ge, *Radiat. Phys. Chem.*, **80**, 567 (2011).
6. Y. Wattanodorn, R. Jenkan, P. Atorngitjawat and S. Wirasate, *Polym. Test.*, **40**, 163 (2014).
7. J. K. Pi, H. C. Yang, L. S. Wan, J. Wu and Z. K. Xu, *J. Membr. Sci.*, **500**, 8 (2016).
8. G. Zhang, S. Lu, L. Zhang, Q. Meng, C. Shen and J. Zhang, *J. Membr. Sci.*, **436**, 163 (2013).

9. L. Yan, Y. S. Li and C. B. Xiang, *Polymer*, **46**, 7701 (2005).
10. C. Yao, X. S. Li, K. G. Neoh, Z. L. Shi and E. T. Kang, *J. Membr. Sci.*, **320**, 259 (2008).
11. Y. F. Yang, H. Q. Hu, Y. Li, L. S. Wan and Z. K. Xu, *J. Membr. Sci.*, **376**, 132 (2011).
12. Q. Gu and Z. Jia, *React. Funct. Polym.*, **73**, 1114 (2013).
13. Y. F. Yang, Y. Li, Q. L. Li, L. S. Wan and Z. K. Xu, *J. Membr. Sci.*, **362**, 255 (2010).
14. R. Yang, H. Jang, R. Stocker and K. K. Gleason, *Adv. Mater.*, **26**, 1711 (2014).
15. T. Xiang, C. D. Luo, R. Wang, Z. Y. Han, S. D. Sun and C. S. Zhao, *J. Membr. Sci.*, **476**, 234 (2015).
16. Y. Mei, C. Yao, K. Fan and X. Li, *J. Membr. Sci.*, **417**, 20 (2012).
17. Z. X. Zhou, D. F. Wei, Y. Guan, A. N. Zheng and J. J. Zhong, *J. Appl. Microbiol.*, **108**, 898 (2010).
18. M. Adib, M. Mahdavi, M. A. Noghani and P. Mirzaei, *Tetrahedron Lett.*, **48**, 7263 (2007).
19. E. B. Anderson and T. E. Long, *Polymer*, **51**, 2447 (2010).
20. C. Hamit, Y. Elvan and Y. Osman, *Carbohydr. Polym.*, **69**, 318 (2007).
21. M. W. Sabaa, N. A. Mohamed, R. R. Mohamed, N. M. Khalil and S. M. A. E. Latif, *Carbohydr. Polym.*, **79**, 998 (2010).
22. B. Gupta, N. Anjum, S. K. H. Gulrez and H. Singh, *J. Appl. Polym. Sci.*, **103**, 3534 (2007).
23. P. Kleyil, V. Jacobs, C. K. Na, C. L. Frost, Z. R. Tshentu and N. Torto, *Int. J. Polym. Mater. Polym. Biom.*, **64**, 287 (2015).
24. I. Melendez-Ortiz, H. C. Alvarez-Lorenzo, A. Concheiro, V. M. Jimeenez-Paaez and E. Bucio, *Radiat. Phys. and Chem.*, **119**, 37 (2016).
25. C. K. Na and H. J. Park, *Appl. Polym.*, **116**, 2723 (2010).
26. J. A. Schwarz, C. T. Driscoll and A. K. Bhanot, *J. Colloid Interface Sci.*, **24**, 55 (1997).
27. H. Ma, R. H. Davis and C. N. Bowman, *Polymer*, **42**, 8333 (2001).
28. M. Takafuji, S. Ide, H. Ihara and Z. Xu, *Chem. Mater.*, **16**, 1977 (2004).
29. H. El-Hamshary, M. M. G. Fouda, M. Moydeena, M. H. El-Newehy, S. S. Al-Deyab and A. Abdel-Megeed, *Int. J. Biol. Macromol.*, **72**, 1466 (2015).
30. D. O. Hummel and F. Scholl, Atlas of Polymer and Plastic Analysis, Hanser, Munich, 2nd Ed. (1990).